2024-09

CFD Analysis of Flow Characteristics and Diagnostics of Leaks in Water Pipelines

Mushumbusi, Philbert

ETASR

https://doi.org/10.48084/etasr.8146

CFD Analysis of Flow Characteristics and Diagnostics of Leaks in Water Pipelines

Philbert F. Mushumbusi
School of Computational and Communication Science and Engineering, Nelson Mandela African Institution of Science and Technology, Tanzania | Department of Mathematics and Statistics, College of Natural and Mathematical Sciences, The University of Dodoma, Tanzania
mushumbusip@nm-aist.ac.tz (corresponding author)

Ashvinkumar Chaudhari
Department of Computational Engineering and Analysis, Turku University of Applied Sciences, Turku, Finland
ashvin.chaudhari@turkuamk.fi

Judith Leo
School of Computational and Communication Science and Engineering, Nelson Mandela African Institution of Science and Technology, Tanzania
judith.leo@nm-aist.ac.tz

Verdiana G. Masanja
School of Computational and Communication Science and Engineering, Nelson Mandela African Institution of Science and Technology, Tanzania
verdiana.masanja@nm-aist.ac.tz

Received: 15 June 2024 | Revised: 11 July 2024 | Accepted: 13 July 2024

 DOI: https://doi.org/10.48084/etasr.8146

ABSTRACT

This study utilizes Computational Fluid Dynamics (CFD) to generate pressure and flow rate values for the analysis of flow characteristics and the diagnosis of leaks in inclined pipelines. The Semi-Implicit Method for Pressure-Linked Equations (SIMPLE) solver in OpenFOAM software was modified to incorporate the effect of pipe orientation angle. Subsequently, the SIMPLE solver was employed to simulate the flow of water through the pipe. Leakage rates were observed to vary in magnitude with respect to leak position and pipe orientation angle, except that leaks close to the flow inlet and pipes with a greater inclination were associated with higher leakage rates. A mathematical leak model is proposed based on non-dimensional flow variables and pipe orientation angle. To generate sufficient pressure values and leakage rates, the CFD simulation was performed 70 times. These values were then incorporated into the mathematical model for the leak location to be predicted. The proposed method is applicable to the detection of leakages of varying sizes in pipelines with different orientations. Therefore, knowing the pipe orientation angle and measurements of inlet flow rate, outlet flow rate, and pressure drop, the model can be used to precisely locate leaks in a pipeline.

Keywords-CFD; incompressible flow; leakage; openFOAM; turbulent flow

I. INTRODUCTION

Leakages in underground pipeline networks deployed for the transportation of potable water are often the result of a number of factors, including the age of the infrastructure, corrosion, poor installation practices, destructive human activities, natural catastrophes, and abrupt pressure fluctuations. Such leaks not only result in the loss of treated water [1], but if not detected and repaired in a timely manner, can also lead to significant economic losses, environmental destruction [2], and public health problems [3]. The analysis of scenarios involving leak flow rates and pressure drops, particularly in relation to changes in pipeline orientation, and the development of methods for the detection and location of leaks can lead to a substantial enhancement of the safety of the pipeline system. A variety of theoretical and experimental studies have been carried out with the objective of developing methods that can assist system operators in the mitigation of

pipe leaks and other forms of damage. These methods can be broadly classified into two main categories: hardware-based and software-based, as discussed in [4]. Hardware-based methods, which include the use of acoustic loggers, fiber optics, cable sensors, ground-penetrating radar, liquid sensing tubes, and smart balls, entail a physical inspection of the pipelines in order to detect and locate any leakage. In contrast, software-based methods do not necessitate physical inspection, but rely on real-time monitoring of fluid flow dynamics and internal pipeline characteristics [5]. Examples of software-based methods involve mass/volume balance, transient modeling, pressure analysis, statistical analysis, the Internet of Things (IoT), and Artificial Intelligence (AI) algorithms. Mathematical models can be grouped into two principal categories: steady-state models [6], which assume that flow conditions and properties remain constant over time, and transient (unsteady-state) models [7], which are based on a time-dependent analysis of fluid properties and flow conditions.

In the 21st century, significant advances in computational power and computer software have enabled the pervasive application of CFD for the analysis of fluid hydrodynamic behavior. This progress has established the basis for the development of technologies capable of detecting and locating anomalies in pipelines. Over the past decade, numerous studies, as summarized in Table I, have employed CFD techniques to make significant contributions to the diagnosis of leaks in fluid pipelines [8]. These studies frequently use Reynolds-averaged Navier-Stokes (RANS) equations and three-dimensional turbulent models, which enables the detection of the smallest leakages and the precise pinpointing of their locations. However, there is a paucity of knowledge regarding the impact of pipe orientation angle on flow characteristics and its influence on leakages in the context of single-phase flow.

Authors in [9] employed CFD simulations of the two-equation k-ε transport model to examine the characteristics of a single leak under both steady and unsteady turbulent flow conditions. The analysis of state variables revealed the occurrence of abrupt changes in pressure and velocity in the vicinity of the leak. For leak rates of up to 1 lt/min, the line pressure signature was undetectable, whereas the pressure gradient signature was discernible. In [10], CFD was employed to investigate critical flow variables in water pipeline networks, with the objective of developing effective leak detection methods. The results demonstrated that the pressure gradient and flow acceleration were discernible, thereby establishing them as reliable indicators for leak detection methods. Furthermore, the CFD findings were validated through experimentation with dynamic pressure transducers, yielding results that were consistent with the CFD simulations. Authors in [11] used a pipe with two leak holes at different locations to investigate the velocity and pressure fields of oil flow under the emergence of a leak when another leak already existed. The analysis demonstrated that the pressure at the inlet section remained constant regardless of the duration of the leaks or the inlet velocity. Similarly, a systematic numerical analysis of leakage characteristics for incompressible flow was carried out in [12] to examine the influence of diverse flow parameters, including the inlet mass flow rate, leakage pipe diameter, and pipe length. In the performed analysis, the inlet mass flow rate and the leakage pipe diameter (expressed as an area ratio) were identified as the primary factors influencing pressure change at the leak vicinity. Authors in [13] introduced dimensionless variables for leak position, leak rate, and pressure drop with the objective of studying pressure distribution along the pipe in case of no leak and when a leak occurs. The CFD results demonstrated that both the leak rate and location exert a considerable influence on the pressure distribution along the pipe. The authors concluded that the proposed dimensionless variables can be employed to identify the location of leaks in actual pipeline networks. In [14], multiple leakages in the pipeline were diagnosed and it was found that the method can identify and locate the leaks within a short time interval when the pressure and flow rate at the inlet and outlet of the leaking pipe are known. In a more recent study, [15], the influence of leak geometry on the characteristics of flowing water inside the pipe, was studied experimentally and numerically. In comparison, the pressure and velocity fluctuations resulting from circular and square-shaped cracks exhibited similar patterns, but differed from those caused by the slot-shaped crack. The researchers concluded that the shape and size of the leak affect the pressure and velocity profiles in the vicinity of the leak. Furthermore, they found that different crack geometries with the same dimensions exhibit similar curve trends with varying peaks.

TABLE I. COMPARATIVE CFD WORKS CONDUCTED TO ANALYZE LEAKAGES IN FLUID TRANSPORT PIPELINE

Reference	Pipeline	Software	Research objectives	Investigation Parameters
[2]	Subsea	Ansys	Single- and double-holes leaks analysis	Fluid velocity, pressure distribution
[9]	Water	Ansys	CFD simulations of small leaks	Flow rate, pressure distribution, pressure gradient
[11]	Oil	Ansys	Single or double leaks analysis	Fluid velocity, pressure distribution
[12]	Water	Ansys	Investigating leakage characteristics detection model	Mass flow rate, pressure change, pressure gradient
[13]	Oil	Ansys	Developed single leak detection model	Pressure drops, leak flow rate, leak location
[16]	Water	Ansys	Examined flow behavior and detection of probable leakages in a 90-degree pipe elbow	Velocity, pressure, vibration signal
[17]	Oil and Gas	Ansys	Examined flow characteristics around virtual small leaks	Pressure, turbulent kinetic energy, velocity
[18]	Gas	Ansys	Transient simulation for one and two leakage flows in a gas pipeline	Dynamic Pressure
[19]	Water	COMSOL	Investigating the effect of leak geometry	Fluid velocity, pressure distribution

A comprehensive review of the abundant literature on fluid flow in conduits reveals that pressure drop is a crucial

parameter across various fields, including fluid mechanics, thermodynamics, and mechanical engineering. This parameter has a significant impact on system design, efficiency, safety, and reliability. In practical applications, the orientation of pipelines is dependent on the topography of the surrounding residential areas, which are characterized by a range of terrain grades. The orientation of the pipeline can influence the flow rate and pressure drop, which in turn can impact the functionality of the system in the presence of leaks. In response to a more comprehensive understanding of fluid flow characteristics in developing leak detection methods, it is essential to conduct a thorough CFD simulation for different pipe orientation angles and to study the flow characteristics as they impact pressure and flow rate values. Therefore, the present study has evaluated the impact of leak location and leakage rates on pressure drop and flow rates as the pipe orientation angle changes. Furthermore, dimensionless values have been employed for the detection and location of leaks in water pipelines. The use of dimensionless variables for diagnosing leaks and accounting for pipe orientation effects represents a significant advancement compared to traditional methods.

II. MATHEMATICAL MODEL AND CFD SIMULATIONS

A. Navier-Stokes Equations

The equations that describe the properties and flow characteristics of fluids are nonlinear differential equations derived from the fundamental conservation principles of mass and momentum. The general form of mass conservation is expressed by the continuity equation:

$$\frac{D\rho}{Dt} + \rho\frac{\partial u_k}{\partial x_k} = 0 \quad (1)$$

where p is fluid density, t is time, and u_k is fluid velocity in the x_k spatial coordinate (with k= 1, 2, 3).

The conservation of momentum is derived from Newton's second law of motion. In the case of an isotropic, homogeneous, and Newtonian fluid, the momentum conservation equation is expressed in terms of the velocity fields coupled with a pressure term:

$$\rho\frac{Du_i}{Dt} = \rho f_i - \frac{\partial P}{\partial x_i} - \frac{\partial}{\partial x_k}\left(\lambda\frac{\partial u_k}{\partial x_k}\right) + \frac{\partial}{\partial x_j}\left[\mu\left(\frac{\partial u_i}{\partial x_j} + \frac{\partial u_j}{\partial x_i}\right)\right] \quad (2)$$

where f is the force, such as gravity, acting on the fluid, P is the thermodynamic pressure (or static pressure for motionless fluid), ρ and μ are density and dynamic viscosity of fluid, respectively, with $\lambda \approx -\frac{2}{3\pi}$.

Equations (1) and (2) for the analysis of fluid flow characteristics necessitate the introduction of supplementary parameters and assumptions to mitigate the intricacy of fluid flow problems, thereby facilitating the application of theoretical and computational methodologies to ascertain solutions. An incompressible Newtonian fluid in a steady state and fully developed turbulent flow, with the influence of gravity is considered. These assumptions facilitate the reduction of the complex nature of fluid dynamics, thereby enabling the derivation of solutions through theoretical and computational approaches.

B. Turbulence Models

Turbulent flow is defined as a state of chaotic and irregular fluid motion, which is characterized by the presence of eddies and vortices of varying sizes. This phenomenon occurs at high Reynolds numbers (Re), with typical values exceeding 4,000 for flow in pipes. The RANS equations are a specific set of time-averaged equations of motion employed for the modeling of turbulent flows. In the context of steady-state flow of water in pipes, the RANS equations comprise the following equations, which are derived from (1) and (2), respectively:

$$\frac{\partial u_i}{\partial x_j} = 0 \quad (3)$$

$$\frac{\partial}{\partial x_j}(u_i u_j) = g\sin\theta - \frac{1}{\rho}\frac{\partial P}{\partial x_i} + \frac{\partial}{\partial x_j}\left[\frac{\mu}{\rho}\left(\frac{\partial u_i}{\partial x_j} + \frac{\partial u_j}{\partial x_i}\right)\right] - \frac{\partial}{\partial x_j}\left(-\overline{u_i' u_j'}\right) \quad (4)$$

where g is the acceleration due to gravity, θ is the pipe orientation angle, and $\left(-\overline{u_i' u_j'}\right)$ is the Reynolds stress tensor, responsible for the mechanism of turbulent kinetic energy.

RANS equations necessitate further analysis due to the Reynolds stress tensor term, which represents a significant challenge in turbulence flow modeling. Models have been proposed in the literature for the closure of RANS equations, which include the two-equation model (k-ε, k-ω) [20], Large Eddy Simulations (LES) [21], and others [22]. Here, the k-ε turbulent model equations, which are widely used due to their favorable convergence properties, relatively low computational memory requirements, and simplicity in computing turbulent viscosity are employed, using the Boussinesq hypothesis:

$$-\overline{u_i' u_j'} = \upsilon_t\left(\frac{\partial u_i}{\partial x_j} + \frac{\partial u_j}{\partial x_i}\right) - \frac{2}{3}k\delta_{ij} \quad (5)$$

where υ_t is turbulent viscosity and δ_{ij} is the Kronecker symbol. The standard k-ε model transport equations, one associated to the turbulence kinetic energy k, and the other to the turbulence dissipation rate ε, are the following:

$$\frac{\partial}{\partial x_j}(k u_j) = \frac{\partial}{\partial x_j}\left[\left(\upsilon + \frac{\upsilon_t}{\sigma_k}\right)\frac{\partial k}{\partial x_j}\right] + \tau_{ij}\frac{\partial u_i}{\partial x_j} - \epsilon \quad (6)$$

$$\frac{\partial}{\partial x_j}(\epsilon u_j) = \frac{\partial}{\partial x_j}\left[\left(\upsilon + \frac{\upsilon_t}{\sigma_\epsilon}\right)\frac{\partial \epsilon}{\partial x_j}\right] + C_{1\varepsilon}\frac{\epsilon}{k}\tau_{ij}\left(-\overline{u_i' u_j'}\right) - C_{2\varepsilon}\frac{\varepsilon^2}{k} \quad (7)$$

where the relationship between turbulent eddy viscosity υ_t, turbulent kinetic energy k, and the dissipation rate ε, are given:

$$\upsilon_t = C_\mu\frac{k^2}{\epsilon},\ \tau_{ij} = \upsilon\left(\frac{\partial u_i}{\partial x_j} + \frac{\partial u_j}{\partial x_i}\right) \quad (8)$$

Some model constants have the following default values: $C_\mu = 0.009$, $C_{1\varepsilon} = 1.44$, $C_{2\varepsilon} = 1.92$, $\sigma_k = 1$, and $\sigma_\varepsilon = 1.3$.

C. Computational Domain and Mesh Considerations

CFD simulations are generally conducted in three main stages: pre-processing, simulation, and post-processing. The pre-processing stage involves defining the geometry, setting boundary conditions, generating the mesh, and establishing solver parameters. The simulation stage focuses on running simulations using the prepared model. In the post-processing stage, results are extracted from the simulations, graphs are plotted, and discussions are carried out. All activities in this study were conducted using OpenFOAM [23], a free open-source software. A pipe geometry of length 2.5 meters and diameter 0.5 meters was prepared utilizing a blockMeshDict file, with a small leak hole 1.68×10^{-4} m² positioned on top of the pipe. The mesh cells were generated employing the built-in blockMesh utility of OpenFOAM, resulting in a hexahedral mesh comprising 680,000 cells with a maximum skewness of 0.501127. It is essential to establish appropriate Boundary Conditions (BCs) for the CFD solver in order to conduct accurate numerical simulations. Figure 1 shows the geometry and prescribed BCs, while Figure 2 provides a zoomed view of the meshed pipe and a leak hole that is very small and cannot be easily discerned. A variety of inlet-outlet BCs combinations is possible. The one implemented here is a velocity inlet and pressure outlet BC. At the pipe inlet, the flow rate was set to 1.96×10^{-2} m²/s, while atmospheric gauge pressure (zero static pressure) was specified at both the pipe outlet and the leakage point. Furthermore, the standard no-slip boundary condition, which assumes that the fluid velocity relative to the wall is zero, was enforced at the pipe wall.

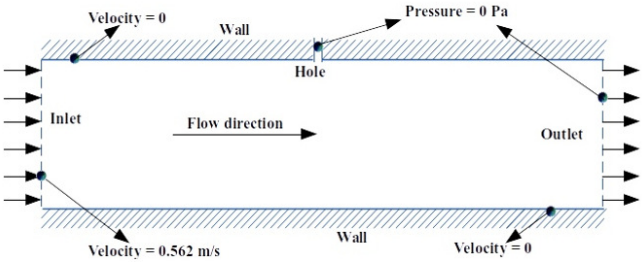

Fig. 1. Boundary conditions and 2D view of the pipe geometry with a hole positioned on top of the pipe.

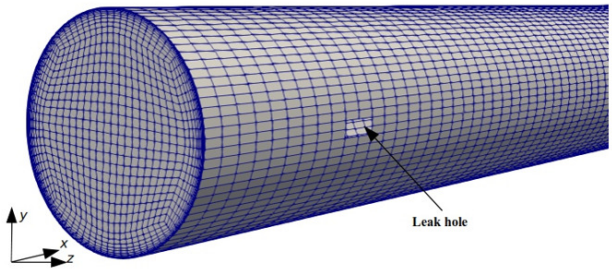

Fig. 2. View of the hexahedral mesh and a leak hole on the side of the pipe.

OpenFOAM software employs the Finite Volume Method (FVM) as the underlying numerical technique [24]. The flow solver deployed is the SIMPLE algorithm, a pressure-based solver that exploits the interrelationship between velocity and pressure to enforce mass conservation, thereby determining the pressure and flow rate fields. This method is particularly effective for handling incompressible flows, where the coupling between velocity and pressure is of critical importance for achieving accurate simulations. The algorithm converges towards a solution that satisfies both the continuity and momentum equations. It should be noted, however, that the simpleFoam steady-state solver for incompressible turbulent flows does not inherently incorporate the effect of gravitational acceleration. Consequently, in order to consider the angle effects in the present work, it was necessary to modify the existing solver by adding a source term representing a constant gravitational effect that would persist throughout the domain. Convergence is achieved when the residuals, which are monitored during the numerical solution of algebraic equations, fall below the predefined convergence criteria that have been set within the solver files.

III. RESULTS AND ANALYSIS

A. Mesh Independence Test

A systematic and comprehensive technique is proposed for conducting a mesh independence test to ensure the accuracy and reliability of a CFD model. The objective of this test is to eliminate or minimize the influence of the mesh size on the outcomes, thereby allowing to disregard the error resulting from numerical approximations. The four mesh development options presented, were tested for the pipe dimensions indicated in Figure 1, without a leak hole. These options were essentially achieved by assigning the mesh size in the axial, radial, and circumferential directions of the pipe geometry, which was defined using the blockMeshDict file. The test was applied to pressure and flow rate values as the flow progressed from the inlet to the outlet of the pipe. Table II contains the pressure drop and flow rate values obtained from each mesh size.

TABLE II. MESH SENSITIVITY ANALYSIS

Mesh	Cells	Maximum Skewness	Pressure Drop (Pa)	Flow rate (m^3/s)
Mesh 1	325,000	0.5167	3,289	0.019611
Mesh 2	680,000	0.5011	3,269	0.019618
Mesh 3	1,025.000	0.5428	3,266	0.019621
Mesh 4	1,444.000	0.5379	3,265	0.019621

Figures 3 and 4 display the variations in pressure gradient and velocity magnitude along the pipe centerline. Upon comparison and analysis of the results, it becomes evident that meshes 2, 3, and 4 yielded nearly identical maximum values of pressure gradient and velocity magnitude. Following a comprehensive assessment of the simulation outcomes, it was determined that mesh 2 was the optimal choice for conducting the remaining simulations. In addition to producing results that were reasonably accurate, this mesh also required fewer computational resources than meshes 3 and 4.

B. Comparison with Experimental Results

The experimental data and CFD simulations presented in [13], were employed to validate the proposed CFD model through a comparison of the resulting data. In the experiment

carried out in that study, a chlorinated polyvinyl chloride pipe with a length of 2.032 m and internal and external diameters of 0.019 m and 0.022 m, respectively, was utilized. To ensure the accuracy of the pipe geometry measurements, the pipeline length, diameter, leak size, and leak location were measured on three separate occasions. Furthermore, three trials were carried out to ascertain the pressure, velocity, and temperature prior to the experiment, with variations of less than 4% among the repeated trials. The experimental findings are therefore considered to be of high quality and reliability, and thus suitable for validating the CFD modeling presented in this research.

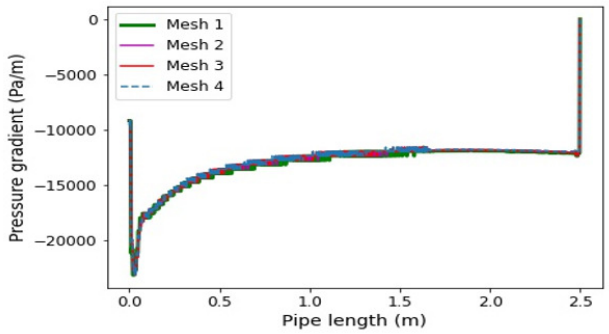

Fig. 3. Pressure gradient profile along the centre-line of the pipe with same inlet flow rates for four different mesh grids in Table I.

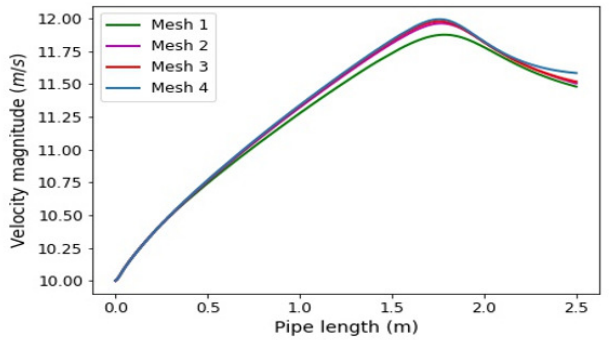

Fig. 4. Velocity profile along the centre-line of the pipe with same inlet flow rates for four different mesh grids in Table I.

For the purpose of comparison, a flow pipe was tilted horizontally and a leak hole was positioned on its upper side, while the boundary conditions presented in Figure 1 were maintained. The simulation process was repeated six times, with each iteration representing a different leak location along the flow pipe, evenly spaced apart. For the comparison and analysis of flow phenomena to be facilitated, the working parameters were expressed as non-dimensional quantities. Figure 5 provides a comparison of the experimental results (*Exp*) and the numerical results (*Num*). This comparison demonstrates a close correspondence, with percentage error variations ranging between 0.74% and 1.76%. These variations were computed using:

$$Error\% = \frac{|Exp - Num|}{Exp} \times 100 \quad (9)$$

C. Velocity and Pressure Contour in the Vicinity of the Leak

Figure 6 visually represents the velocity contours within the pipe and in the surrounding area. In the vicinity of a leak, an increase in velocity is typically observed as a result of the escaping fluid. Moreover, the same figure compares three contours from different pipe orientation angles, thereby demonstrating that the pipe inclination angle affects the flow characteristics of the fluid and the leakage intensity

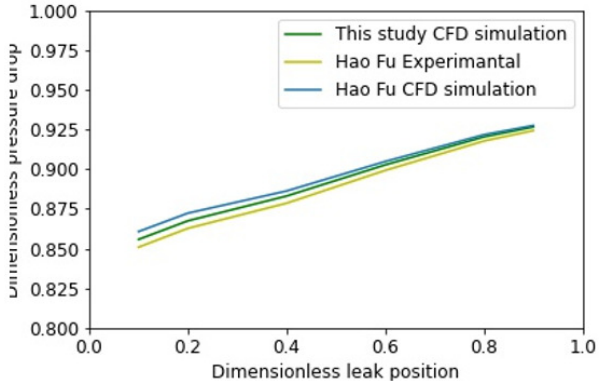

Fig. 5. Comparison of CFD results and experimental results.

This is in accordance with the findings of studies that have identified pipe size and leak geometry and size, as factors that influence the aforementioned characteristics [15]. The magnitude of the flow velocity is greater at the center of the leak hole and diminishes to zero at the pipe wall. Conversely, the pressure magnitude is higher at the pipe inlet, gradually decreasing along the length of the pipe until it reaches a value similar to the pressure boundary condition specified at the leak hole and pipe outlet, as shown in Figure 7.

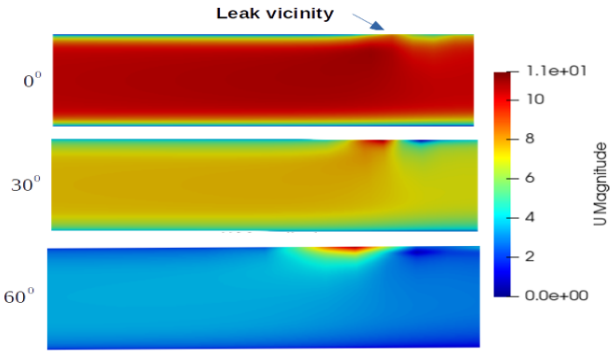

Fig. 6. Velocity magnitude pattern for a pipe inclined at 0^0, 30^0 and 60^0 angles with a leak at 0.5 m from the pipe inlet.

A clear pattern emerges when the velocity and pressure magnitudes are compared. In instances where the pipe is inclined at shallower angles, the velocity distribution within the pipe is markedly elevated. This phenomenon is consistent with the observation that the pressure magnitude is lower in these scenarios. Conversely, when pipes are inclined at steeper angles, the flow velocity is notably low, which coincides with the trend of high-pressure magnitudes in such cases. The

magnitude of velocity and pressure can be employed as quantitative measures of the severity of leakage.

D. The Influence of Leak Location on Leakage Rate and Pressure Drop Along the Pipe Flow

The location of a leak along the pipeline has a substantial impact on both the leakage rate and the pressure drop. Figure 8, exhibits considerable discrepancies in leakage rates, as a consequence of alterations in the position of the leak and the angle of the pipe's orientation. A higher leakage rate is observed in the pipeline system when the leak occurs in the vicinity of the inlet section. As the leak point is relocated along the pipeline, the leakage rate exhibits a gradual decline, with the magnitude of leakage becoming increasingly diminished in proximity to the outlet section.

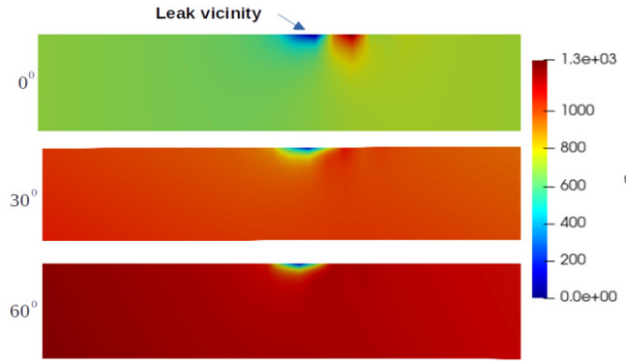

Fig. 7. Pressure magnitude pattern for a pipe inclined at 0^0, 30^0 and 60^0 angles with a leak at 0.5 m from the pipe inlet.

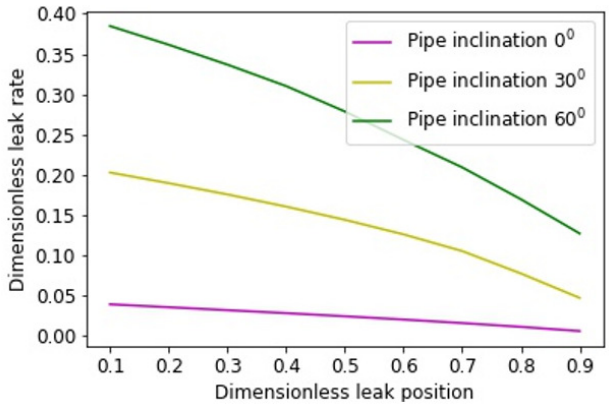

Fig. 8. The influence of leak position on leakage rates as the pipe orientation angle changes.

A comparison of the leakage intensity between shallower and steeper inclined pipes reveals that leakage at low orientation angles is less than the one at steeper angles, as evidenced in Figure 9. In this case, the leakage in a horizontal pipe is taken as a reference point for the calculation of the difference in leakage rates (expressed as a percentage) for pipes inclined at 30 and 60 degrees. It was determined that the discrepancy in leakage rate can vary between 4% and 16% for pipe orientation angles between 0 degrees and 30 degrees, or between 12% and 34% for angles between 0 degrees and 60 degrees. It is crucial to acknowledge that a twofold increase in pipe orientation angle results in a twofold increase in leakage rate. However, a fixed-size leak geometry exhibits diverse leakage rates when situated at varying positions along the pipe and when the pipe orientation angle undergoes alteration. This introduces complexity during the development of Leak Detection Methods (LDM), indicating the necessity for the formulation of a mathematical model that incorporates a parameter for pipe orientations to enhance the leakage detection process.

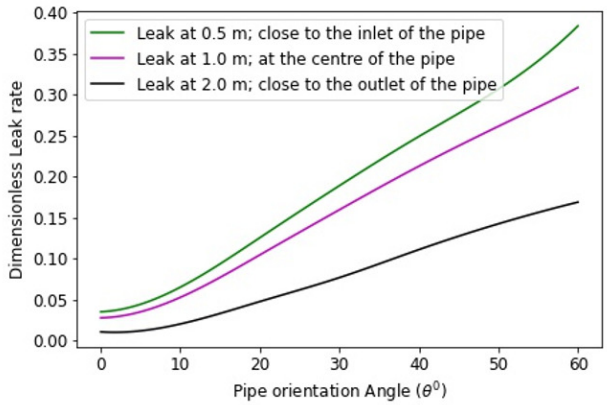

Fig. 9. Comparison of leakage rates at different leak locations as the pipe orientation angle changes.

Figure 10 demonstrates that when a leak occurs in the vicinity of the inlet section of the pipe, the pressure drop is relatively minimal.

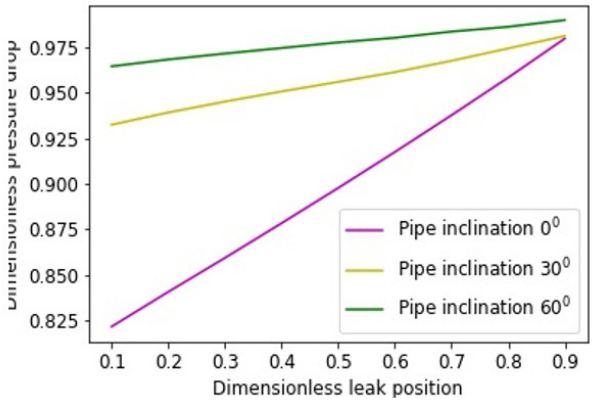

Fig. 10. Comparison of pressure drop in the pipeline as the leak location varies along the flow direction for different pipe orientation angles.

However, as the leak position approaches the outlet section, the pressure drop increases. A comparison of the three curves, representing different leak scenarios, reveals that the horizontal pipe (0 degrees angle) initially exhibits the lowest pressure drop, but this value increases rapidly along the length of the pipe. In contrast, for inclination angles of 30 and 60 degrees, the pressure drop is relatively high at the inlet section in

comparison to the horizontal pipe. Nevertheless, it increases at a relatively moderate rate towards the outlet section. The data clearly indicate that the pressure drop increases as the inclination angle rises and the leak position moves further from the inlet section, regardless of the pipe orientation angle. The pressure in the pipeline is higher at the inlet and varies with the pipe angle. This means that the water requires different pumping power to move through. An increase in pipe orientation angle results in a notable intensification of flow resistance, necessitating a greater input of energy to overcome gravitational forces. This, in turn, gives rise to augmented frictional losses and turbulence along the pipe length. As a result, the impact on flow characteristics is evident in the form of a heightened pressure drop, which in turn amplifies the leakage flow rate.

The findings presented in Figures 8, 9, and 10 offer valuable insights into the relationship between pipeline orientation, leakage rate, leak location, and pressure drop. A comprehension of these dynamics is imperative for the assessment and management of pipeline integrity, the optimization of maintenance strategies, and the mitigation of potential risks associated with pipe leaks. A mathematical model is proposed in an attempt to further analyze the relationships between these key parameters in the context of leakage modeling.

IV. MATHEMATICAL MODEL FOR PREDICTION OF SINGLE LEAK IN ELEVATED PIPELINE

A Gaussian function formulated using dimensionless leakage location L_d, dimensionless leakage flow rate Q_d, and dimensionless pressure drop P_d, is defined as:

$$L_d = \frac{L^*}{L}, \quad Q_d = \frac{Q^*}{Q}, \quad P_d = \frac{P^*}{P} \tag{10}$$

where L is the pipe length, L^* is the leak location from the inlet section of the pipe, Q is the inflow rate, Q^* is the leakage rate, P and P^* are the pressure drop in the absence and presence of a leak in the pipeline respectively, and

$$P_d = P_0 + A \cdot exp\left(\frac{1}{2}\left[\frac{(L_d - x_c)\cdot\cos\theta + (Q_d + y_c)\cdot\sin\theta}{w_1}\right]^2 - \frac{1}{2}\left[\frac{(-L_d + x_c)\cdot\sin\theta + (Q_d - y_c)\cdot\cos\theta}{w_2}\right]^2\right) \tag{11}$$

where P_0 denotes the base pressure drop due to friction and other factors independent of flow rate and leakage rate, A is the amplitude of the pressure drop, x_c and y_c control the horizontal shift of the centre (peak) of the Gaussian function, while w_1 and w_2 are the widths of the Gaussian curves describing the dependence of pressure drop on the distance from the leak point in the longitudinal and transverse directions, respectively. Equation (11) includes an angle θ for pipe orientations. This inclusion ensures that when θ is set to zero, (11) is simplified to a mathematical model presented in previous work [13], for the prediction of a single leak point in a horizontal pipe. The first component signifies the effect of the leak location on pressure drop along the pipe's length, while the subsequent component characterizes the impact of the leakage flow rate on pressure drop. This study introduced pipeline elevation angle in order to discuss its influence on both leakage flow rate and pressure drop, which are essential parameters for the detection and location of leaks. This model enables the identification of the leak location when the pressure difference and flow rate values are known. The values are generated using six different inlet flow rates and are then transformed into dimensionless values before being incorporated into the proposed mathematical model by deploying a neural network method, Artificial Neural Networks for Scientific Computations (SciANN), which is an open-source neural network library [25], built on the widely used deep learning frameworks, TensorFlow and Keras. The initial coefficients for this Gaussian function were adopted from [13], resulting in an adjusted R-squared value of 0.98.

Figure 11 showcases a graphical representation of the pressure drop as a function of the leakage position and leak flow rates. The proximity of the leak location to the pipe inlet is directly correlated with the leak rate, which in turn is inversely proportional to the pressure. This suggests that when a leak occurs at a considerable distance from the pipeline inlet, the pressure drop is greater, reducing the flow velocity and consequently leading to a lower leak rate. Conversely, when the leak occurs in close proximity to the inlet, the pressure drop is lower, resulting in a higher leak rate. Once (11) is successfully fitted to the data, it can be utilized to estimate the leak location along the pipe, provided that the pressure drop and flow rate measurements have been accurately collected.

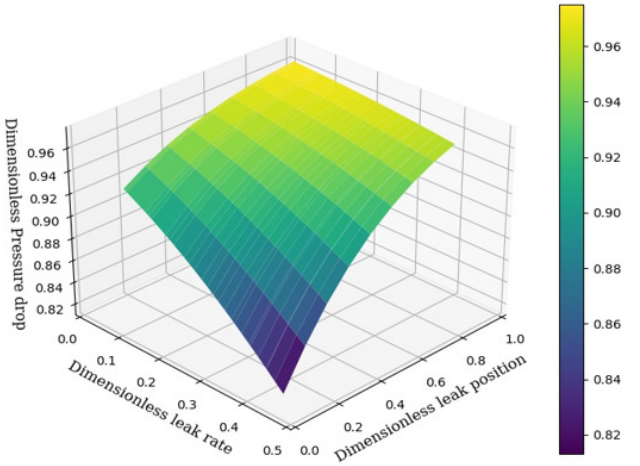

Fig. 11. Graphical depiction of non-dimensional pressure drop with leakage flow rates and leak position.

V. CONCLUSION

A mathematical model is proposed for the diagnosis of pipeline leakage based on the use of dimensionless variables, leakage rate, leak location, and pressure drop. The model is developed to take into account the effects of pipe orientation during fluid flow. The study examined the interrelationship between flow parameters, leading to the following conclusions:

- A non-linear relationship exists between leakage flow rate and pressure drop as the pipe orientation angle is altered. An increase in the pipe orientation angle results in an

elevated leakage rate, which is attributed to the augmented pressure drop within the pipeline.

- The leakage rate is observed to be lower for pipes with a lesser degree inclination ($\theta \leq 30^{o}$) and higher for pipes with a greater degree inclination ($\theta > 30^{o}$), irrespective of the location of the leak along the pipeline.
- The leakage rate is observed to be higher for leaks situated in proximity to the flow inlet and to gradually decrease as the leak hole is relocated towards the pipe outlet, regardless of the pipe orientation angle
- The proposed mathematical model introduces the pipe inclination angle (θ), thus enabling a comprehensive analysis of fluid flow rates and pressure differences influenced by pipeline orientation.

This advancement provides a notable enhancement over preceding models, which are primarily oriented towards horizontal pipelines. When the pipe inclination angle (θ) is zero, the model effectively reverts to the earlier models, thereby demonstrating its versatility and robustness in a variety of pipeline configurations. The model can be used in real-world flow systems for the purpose of locating leaks. However, a number of measurements must be performed, including the inlet flow rate, the outlet flow rate, and the inlet and outlet pressure values. These dimensionless values can be processed and fitted into the proposed equation deploying a variety of curve-fitting methods, including regression, principal component analysis, and neural networks. Once the equation is successfully fitted to the data, it can be employed to identify the location of the leak along the pipeline. It is crucial to note that this model addresses a single leak under steady flow conditions. Consequently, further research is necessary for a model capable of addressing multiple leaks in fluid transport pipelines, including both steady and unsteady flow scenarios to be developed.

REFERENCES

[1] U. P. Shushu, H. C. Komakech, D. Dodoo-Arhin, D. Ferras, and M. L. Kansal, "Managing non-revenue water in Mwanza, Tanzania: A fast-growing sub-Saharan African city," *Scientific African*, vol. 12, Jul. 2021, Art. no. e00830, https://doi.org/10.1016/j.sciaf.2021.e00830.

[2] O. Y. Wei and S. U. Masuri, "Computational fluid dynamics analysis on single leak and double leaks subsea pipeline leakage," *CFD Letters*, vol. 11, pp. 95–107, Jan. 2019.

[3] M. W. LeChevallier, R. W. Gullick, M. R. Karim, M. Friedman, and J. E. Funk, "The potential for health risks from intrusion of contaminants into the distribution system from pressure transients," *Journal of Water and Health*, vol. 1, no. 1, pp. 3–14, Mar. 2003.

[4] J. Stańczyk and E. Burszta-Adamiak, "Development of Methods for Diagnosing the Operating Conditions of Water Supply Networks over the Last Two Decades," *Water*, vol. 14, no. 5, Jan. 2022, Art. no. 786, https://doi.org/10.3390/w14050786.

[5] S. El-Zahab and T. Zayed, "Leak detection in water distribution networks: an introductory overview," *Smart Water*, vol. 4, no. 1, Jun. 2019, Art. no. 5, https://doi.org/10.1186/s40713-019-0017-x.

[6] L. Saidi, S. Mekroussi, S. Kherris, D. Zebbar, and B. Mébarki, "A Numerical Investigation of the Free Flow in a Square Porous Cavity with Non-Uniform Heating on the Lower Wall," *Engineering, Technology & Applied Science Research*, vol. 12, no. 1, pp. 7982–7987, Feb. 2022, https://doi.org/10.48084/etasr.4604.

[7] N. M. C. Martins, A. K. Soares, H. M. Ramos, and D. I. C. Covas, "CFD modeling of transient flow in pressurized pipes," *Computers & Fluids*, vol. 126, pp. 129–140, Mar. 2016, https://doi.org/10.1016/j.compfluid.2015.12.002.

[8] A. Negm, X. Ma, and G. Aggidis, "Review of leakage detection in water distribution networks," *IOP Conference Series: Earth and Environmental Science*, vol. 1136, no. 1, Jan. 2023, Art. no. 012052, https://doi.org/10.1088/1755-1315/1136/1/012052.

[9] R. Ben-Mansour, M. A. Habib, A. Khalifa, K. Youcef-Toumi, and D. Chatzigeorgiou, "Computational fluid dynamic simulation of small leaks in water pipelines for direct leak pressure transduction," *Computers & Fluids*, vol. 57, pp. 110–123, Mar. 2012, https://doi.org/10.1016/j.compfluid.2011.12.016.

[10] R. Ben-Mansour, K. A. Suara, and K. Youcef-Toumi, "Determination of important flow characteristics for leak detection in water pipelines-networks," *Computational Thermal Sciences*, vol. 5, no. 2, pp. 143–151, 2013, https://doi.org/10.1615/ComputThermalScien.2013006301.

[11] M. de Vasconcellos Araújo, S. R. de Farias Neto, A. G. B. de Lima, and F. D. T. de Luna, "Hydrodynamic Study of Oil Leakage in Pipeline via CFD," *Advances in Mechanical Engineering*, vol. 6, Jan. 2014, Art. no. 170178, https://doi.org/10.1155/2014/170178.

[12] Z. Zeng and R. Luo, "Numerical Analysis on Pipeline Leakage Characteristics for Incompressible Flow," *Journal of Applied Fluid Mechanics*, vol. 12, no. 2, pp. 485–494, Mar. 2019, https://doi.org/10.29252/jafm.12.02.28612.

[13] H. Fu, L. Yang, H. Liang, S. Wang, and K. Ling, "Diagnosis of the single leakage in the fluid pipeline through experimental study and CFD simulation," *Journal of Petroleum Science and Engineering*, vol. 193, Oct. 2020, Art. no. 107437, https://doi.org/10.1016/j.petrol.2020.107437.

[14] H. Fu, S. Wang, and K. Ling, "Detection of two-point leakages in a pipeline based on lab investigation and numerical simulation," *Journal of Petroleum Science and Engineering*, vol. 204, Sep. 2021, Art. no. 108747, https://doi.org/10.1016/j.petrol.2021.108747.

[15] M. De Marchis and B. Milici, "Leakage Estimation in Water Distribution Network: Effect of the Shape and Size Cracks," *Water Resources Management*, vol. 33, no. 3, pp. 1167–1183, Feb. 2019, https://doi.org/10.1007/s11269-018-2173-4.

[16] A. A. Abuhatira, S. M. Salim, and J. B. Vorstius, "CFD-FEA based model to predict leak-points in a 90-degree pipe elbow," *Engineering with Computers*, vol. 39, no. 6, pp. 3941–3954, Jun. 2023, https://doi.org/10.1007/s00366-023-01853-4.

[17] M. A. Asri *et al.*, "Flow Characteristics for Leak Detection in Oil and Gas Pipeline Network Using CFD Simulations," *Journal of Design for Sustainable and Environment*, vol. 4, no. 1, pp. 1–8, Apr. 2022.

[18] P. D. Ndalila, Y. Li, C. Liu, A. H. A. Nasser, and E. A. Mawugbe, "Modeling Dynamic Pressure of Gas Pipeline With Single and Double Leakage," *IEEE Sensors Journal*, vol. 21, no. 9, pp. 10804–10810, May 2021, https://doi.org/10.1109/JSEN.2021.3058507.

[19] S. Ali, M. A. Hawwa, and U. Baroudi, "Effect of Leak Geometry on Water Characteristics Inside Pipes," *Sustainability*, vol. 14, no. 9, Apr. 2022, Art. no. 5224, https://doi.org/10.3390/su14095224.

[20] M. W. Khalid and M. Ahsan, "Computational Fluid Dynamics Analysis of Compressible Flow Through a Converging-Diverging Nozzle using the k-ε Turbulence Model," *Engineering, Technology & Applied Science Research*, vol. 10, no. 1, pp. 5180–5185, Feb. 2020, https://doi.org/10.48084/etasr.3140.

[21] V. Vuorinen, A. Chaudhari, and J.-P. Keskinen, "Large-eddy simulation in a complex hill terrain enabled by a compact fractional step OpenFOAM® solver," *Advances in Engineering Software*, vol. 79, pp. 70–80, Jan. 2015, https://doi.org/10.1016/j.advengsoft.2014.09.008.

[22] K. Hami, "Turbulence Modeling a Review for Different Used Methods," *International Journal of Heat and Technology*, vol. 39, pp. 227–234, Feb. 2021, https://doi.org/10.18280/ijht.390125.

[23] J. Fahlbeck, H. Nilsson, and S. Salehi, "A Head Loss Pressure Boundary Condition for Hydraulic Systems," *OpenFOAM® Journal*, vol. 2, pp. 1–12, Jan. 2022, https://doi.org/10.51560/ofj.v2.69.

[24] M. Manafpour and H. Ebrahimnezhadian, "Investigating the Effect of Ramp Geometry on the Flow Characteristics Around Under Pressure Tunnel Aerator Using OpenFoam Open Source Software," *Engineering, Technology & Applied Science Research*, vol. 9, no. 1, pp. 3705–3710, Feb. 2019, https://doi.org/10.48084/etasr.2427.

[25] E. Haghighat and R. Juanes, "SciANN: A Keras/TensorFlow wrapper for scientific computations and physics-informed deep learning using artificial neural networks," *Computer Methods in Applied Mechanics and Engineering*, vol. 373, Jan. 2021, Art. no. 113552, https://doi.org/10.1016/j.cma.2020.113552.